Wear 436-437 (2019) 203004

Contents lists available at ScienceDirect

Wear

journal homepage: www.elsevier.com/locate/wear

The effect of vanadium alloying on the wear resistance of pearlitic rails

W. Solano-Alvarez[a,*], L. Fernandez Gonzalez[b], H.K.D.H. Bhadeshia[a]

[a] Department of Materials Science and Metallurgy, University of Cambridge, UK
[b] Centro Tecnologico IDONIAL, Parque Empresarial PEPA, Calafates, 33417, Aviles, Asturias, Spain

ARTICLE INFO

Keywords:
Pearlite
Vanadium
Rail steel
Grooved rail
Wear resistance

ABSTRACT

Due to the increasing demand on pearlitic rails to support heavier loads and higher speeds, grooved rails for tramways and light rail transit (LRT) require strengthening via alloying or heat treatment, i.e. accelerated cooling after hot-rolling. In this study, the wear performance of five different commercial grades is compared using unlubricated twin-disc testing and detailed microstructural characterisation. Results indicate that the vanadium-alloyed steel experiences *less than half* the wear rate of a heat-treated grade with a similar hardness. This is attributed to the increased stability and toughness of vanadium-containing cementite, as compared to pure cementite. The evidence suggests that vanadium partitions into the cementite lamellae during the formation of pearlite. This improvement in wear resistance due to vanadium could enable an approximately two-fold reduction in the maintenance and life cycle costs relative to heat-treated rail alternatives.

1. Introduction

The demand to subject rails to higher speeds, greater traffic densities, heavier loads, and mixed traffic enhances damage, mainly in the form of wear (loss of rail profile), plastic deformation, corrugation, and rolling-contact fatigue cracking [1]. However, in the case of tramways and light rail transit, the most prominent damage mechanism is wear due to the dense traffic, frequent braking and acceleration of vehicles, sharp turns, and variable loads. A traditional approach to increase the wear resistance is the refinement of the interlamellar spacing of pearlite [2,3], either through alloying or accelerated cooling after rolling, in order to increase the hardness without compromising toughness [4–6]. Accelerated cooling can be achieved using compressed air, but is maximised by using water sprays. However, this can lead to undesired microstructures if water accumulates at cavities in rails with intricate geometries such as grooves. An alternative is to add certain elements such as vanadium or chromium with the aim of increasing the hardness, thus allowing to reduce the carbon content to improve the weldability of the alloys.

Vanadium, in concentrations as small as 0.1 wt%, can increase the hardness by 75 HV [7] and the strength by at least 100 MPa [8,9], albeit with some reduction in ductility and impact resistance [10]. Strengthening by this method can lead to savings by eliminating the costs of head-hardening [8]. Literature suggests that the strengthening mechanism involves the precipitation of sheets of fine vanadium carbide platelets at the ferrite/austenite interfaces [8,10–13] (classically known as interphase precipitation [14,15]). Furthermore, some precipitation occurs at the prior austenite grain boundaries, thereby preventing the formation of a continuous network of proeutectoid cementite [16,17]. Apart from consequences on the interlamellar spacing and allotriomorphic ferrite, the cooling rate can also influence the dispersion parameters of vanadium carbides [8].

The aim of this study is to evaluate and compare the effectiveness that different strengthening approaches have on wear, as well as to reveal the metallurgical mechanisms by which they operate, in order to provide a technical guide that indicates which commercial alloys would allow reductions to the maintenance and life cycle costs of a tramway or light rail transit installation.

2. Experimental methods

2.1. Material and microstructural characterisation

For this study, one standard rail grade without tailored alloying or heat treatment (R260) was selected along with two heat-treated grades (R290GHT and R340GHT, where GHT means *groove heat treated*), and two vanadium containing grades manufactured by *ArcelorMittal*, one low carbon (R290V) and another high carbon and chromium (B1000). The composition of the five different grades compared in this study, listed in Table 1, was obtained through gravimetric analysis in the case of silicon, a *Leco CS230* combustion infrared detection equipment for carbon and sulphur, and atomic emission spectroscopy for the

* Corresponding author.
E-mail address: ws298@cam.ac.uk (W. Solano-Alvarez).

https://doi.org/10.1016/j.wear.2019.203004
Received 2 May 2019; Received in revised form 8 July 2019; Accepted 7 August 2019
Available online 12 August 2019

Table 1
Chemical composition of the grooved rails studied, wt%.

Grade	C	Mn	Si	Cr	V	P	S	H_2
R260	0.62–0.80	0.70–1.20	0.15–0.58	<0.15	–	<0.02	<0.02	<0.00025
R290V	0.45–0.58	1.00–1.25	0.15–0.58	<0.15	0.08–0.20	<0.02	<0.02	<0.00025
R290GHT	0.40–0.55	0.70–1.25	0.15–0.58	<0.15	–	<0.02	<0.02	<0.00020
R340GHT	0.62–0.80	0.70–1.20	0.15–0.58	<0.15	–	<0.02	<0.02	<0.00020
B1000	0.65–0.85	0.90–1.30	0.15–0.58	0.20–0.80	0.05–0.15	<0.02	<0.02	<0.00025
Wheel R7	0.51	0.79	0.31	0.15	0.004	0.010	0.002	–

remaining elements. Due to confidentiality issues by the providers of the steel grades, a range of the actual measured composition of the tested samples is given in order to understand compositional differences without showing the exact values.

After cutting cross-sectional slices ~20 mm thick of each rail, smaller samples from the top right hand corner of the thicker rail head, corresponding to the position for extraction of tensile specimens according to EN 14811 [18], were cut for initial microstructural examination (Fig. 1). Samples were mounted in bakelite, ground, polished to 0.25 μm, etched in 2% nital, and characterised using a *FEI Nova NanoSEM* (scanning electron microscope) to determine the interlamellar spacing and prior austenite grain size, both at the surface and at the matrix (10 mm deep). The true interlamellar spacing was quantified using the stereographic method described in Refs. [19,20] by obtaining 15 different micrographs, each at a magnification of ×20,000. Likewise, the prior austenite grain size was determined using stereography by analysing 10–15 micrographs for each region obtained at magnifications of ×200–500, thanks to the presence of allotriomorphic ferrite that delineates the grain boundaries.

Some samples were then characterised using transmission electron microscopy (TEM) by cutting a 0.5 mm thick slices which were then coated with silver paste, followed by slicing into 3 mm diameter discs using spark erosion. They were then ground to a thickness of ~50 μm using silicon carbide paper, for electropolishing using a *Struers TenuPol 5* twin-jet polishing machine and a solution of 80% ethanol, 15% glycerol, and 5% perchloric acid at 20.5 V and − 5 to 5 °C. TEM samples were charaterised in a *FEI Tecnai Osiris* microscope, with energy dispersive X-ray spectroscopy (EDS) in scanning electron transmission microscopy (STEM) mode using a high-angle annular dark field (HAADF) detector and *FEI Super-X* system employing 4 *Bruker* silicon drift EDS detectors at 200 kV of accelerating voltage.

The rolling surface hardness was determined as described in EN ISO 6506–1 [21] by machining 5 mm off the rail head and indenting it with a Brinell tungsten carbide sphere of 2.5 mm in diameter and a load of 1.839 kN applied during 15 s. The cross-sectional hardness was also determined both at the sub-surface and 10 mm deep, referred to as 'matrix', using an automatic *Qness Q30 A* + by indenting ten times with a 30 kg (HB30) load and a dwell time of 15 s. The hardness of the cementite in samples R290V and R290GHT was measured by micro-indentation using a force of 5 mN (0.5 g) after having spheroidised both samples at 680 °C for 72 h.

2.2. Twin-disc wear testing

Twin disc samples were obtained from the head of each rail at a depth of 5 mm from the running surface ensuring that the rotational axes of the discs were normal to the longitudinal axis of the rail (Fig. 1). Both rail and wheel discs had a diameter of 47 mm, a thickness of 10 mm, and an initial average surface roughness of <1 μm. Two samples per steel grade were run all at room temperature using the same wheel steel with a hardness of 235 HV10 (R7, Table 1). All wear samples were run dry for 100,000 cycles, a load of 750 MPa (1.25 kN), a slip of 2%, and rotated at 400 rpm. The tests were interrupted at 10,000, 25,000, and 50,000 cycles in order to determine weight loss. Rolling contact fatigue tests were not conducted since the predominant damage mechanism in grooved rails is wear, because of the low speeds, frequent braking and acceleration, and low curvature radius of tramways. The custom-made twin disc test rig has two motors to individually activate the rail and the wheel discs, a transducer on the rail-disc axis to determine the friction coefficient between the discs, and a hydraulic piston that can apply a force of up to 15 kN between both discs.

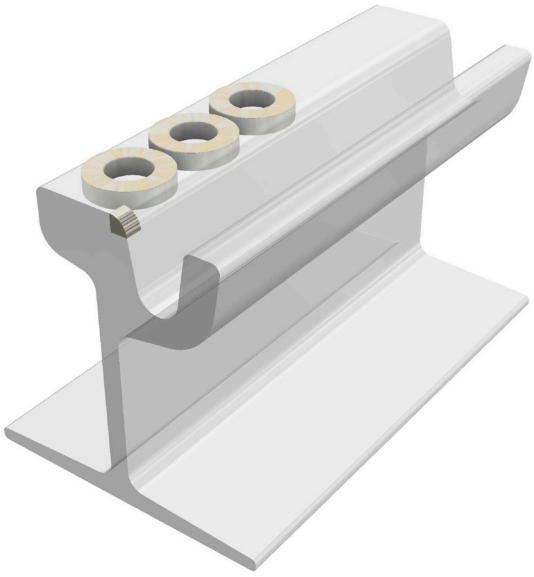

Fig. 1. Schematic of the position where metallographic and twin disc samples were extracted from the grooved rail head.

3. Results and discussion

3.1. Microstructural characterisation

The results of rolling surface hardness (HB187.5), cross sectional hardness (HB30), prior austenite grain size and true interlamellar spacing, are presented in Table 2. For reference, experimental values of ultimate tensile strength (UTS) and elongation of grades R290V and B1000 are presented as well as the minimum values of the norm (EN 14811 [18]) for all other grades.

The values of cross-sectional sub-surface hardness for the air cooled samples (R260, R290V, and B1000) are comparable to those of the matrix (10 mm deep), whereas they are slightly lower than the matrix in the rapidly cooled samples, R290GHT and R340GHT, possibly due to mild decarburisation of the latter. Nevertheless, the cross sectional hardness values of the heat treated samples are more uniform, especially at the rail head. Rolling surface hardness values are up to 10% greater than those in the cross section, most likely due to the grain shape anisotropy caused by rolling and the asymmetry of cross sectional sub-surface hardness indents performed close to an edge that can lead to inaccurate measurements.

The austenite grain size depends not only on the reheating temperature and time but also on the temperature and deformation ratio of each rolling pass. The prior austenite grain size will in turn control the

Table 2
Microstructural data showing average values and standard error with a 95% confidence interval. Matrix values were collected from 10 mm deep and sub-surface data from just below the surface in case of the prior austenite grain size (PAGS) and interlamellar spacing (ILS), but 0.5 mm deep in the case of hardness. The values of prior austenite grain size missing from the table correspond to those samples which did not contain allotriomorphic ferrite decorating the austenite grain boundaries.

Grade	Hardness/HB187.5	Cross-section hardness/HB30		PAGS/ μm		True ILS/nm		UTS/MPa	Elongation/%
	rolling surface	sub-surface	matrix	sub-surface	matrix	sub-surface	matrix	min.	min.
R260	276±2	267±6	265±3	57±4	71±5	227±38	262±38	880	10
R290V	312±6	299±12	299±3	51±2	70±3	197±32	207±29	960	10
R290GHT	308±2	292±2	299±1	48±2	75±6	135±19	162±32	960	10
R340GHT	356±3	344±5	353±2	45±2	–	125±18	119±17	1175	9
B1000	353±8	330±6	322±3	39±2	–	129±20	193±37	1080	9

number density of nucleation sites during the pearlitic transformation, thus influencing the interlamellar spacing, and consequently, the hardness. In all grades, the prior austenite grains at the sub-surface were smaller than in the matrix (10 mm deep) due to the higher deformation ratios experienced at the surface than in the centre of the rail head. Matrix prior austenite grain sizes seem to be comparable amongst all grades, indicating that the role of vanadium here is not that of a grain refiner.

A smaller austenite grain size, should, by enhancing the nucleation rate, raise the pearlite transformation temperature, leading to a coarser interlamellar spacing. However, the faster cooling at the surface, more than compensates for this effect, leading to a finer interlamellar spacing at the sub-surface compared with the matrix. It is worth noting that similar values of interlamellar spacing to those achieved with accelerated cooling can be replicated under standard air cooling by adequate alloying with chromium and silicon as is the case of B1000.

In the context of chemical composition, a small increase in carbon content (R290GHT vs R340GHT) significantly increases hardness, although problems with weldability and proeutectoid cementite may arise in the absence of enhanced silicon concentrations or the application of accelerated cooling [22,23]. To avoid this, alloying with elements such as vanadium can help achieve a high hardness at a lower carbon concentration as seen by comparing the hardness and V content of R290V against R260. Further hardness can be achieved by the addition of manganese as a ferrite strengthener, silicon to suppress proeutectoid cementite formation [24], and chromium to increase the equilibrium transformation temperature[1] as is the case for B1000, without the need to incorporate accelerated cooling.

To reveal the hardening mechanism of vanadium, having discarded its role as a grain refiner, TEM was conducted on R290V at 10 mm from the running surface with the intention of finding a fine distribution of vanadium carbides in the ferrite within the pearlite. As Fig. 2 shows, vanadium carbides could not be found. Interestingly, a fine distribution of copper sulphide (CuS) precipitates was found instead, which although have the right size to provide precipitation strengthening, may not be present in large enough quantities for a macroscopic effect to be felt, due to the low concentration of Cu (0.02 wt%) and S (0.008 wt%) in the alloy. The only regions in which elongated vanadium carbides were found was in the ferrite allotriomorphs Fig. 3. Parsons and Edmonds reported that vanadium carbide precipitation was easily found in the proeutectoid ferrite, but occurred less frequently in the pearlitic ferrite [10]. Pickering and Garbarz also found a lack of interphase precipitation in samples isothermally transformed to pearlite and concluded that vanadium hardening precipitates can often not be present until after an additional aging treatment due to the unavailability of C and N dissolved in the pearlitic ferrite [7].

Dunlop et al. reported that during slow transformation to pearlite, vanadium has time to partition and dissolve into the growing cementite, leaving precipitate-free zones around the cementite lamellae. In rapidly cooled samples, vanadium carbides do precipitate at the interfaces between the cementite lamellae and the ferritic pearlite, but precipitate-free zones can be present too, either because the precipitates are too fine or most likely, due to the transformation proceeding too rapidly for precipitation to take place leaving the vanadium in solid solution [8]. After aging the rapidly cooled sample at 700 °C for 3 h, a large dispersion of vanadium carbides precipitated in the ferritic component of pearlite, leading to the conclusion that neither fast nor slow coolings are ideal, but an intermediate rate is optimum in order to maximise the vanadium carbide precipitation strengthening of ferrite. This work was confirmed by von den Steinen et al. who found that 90% of the vanadium can remain in solid solution in the ferrite if an alloy is rapidly cooled to pearlite, resulting in 5% proeutectoid ferrite, whereas only 50% of the vanadium remained in solution if the alloy was cooled slowly resulting in a mixture of pearlite and 10% proeutectoid ferrite [9]. A simple thermodynamic simulation using the Thermo-Calc Software TCFE9 Steels/Fe-alloys database [26] indicates that indeed under equilibrium conditions (≈ slow cooling), vanadium partitions preferentially to the cementite around 600–700 °C (Fig. 4). Fig. 2 shows that only small residual precipitates are left behind at the centre of the pearlitic ferrite.

Vanadium enrichment of cementite slightly reduces its hardness, but enhances its fracture toughness [27]. Others have concluded that vanadium (and Ti, Nb), make cementite more stable relative to its unalloyed form by decreasing the carbon-dislocation interaction and strengthening of the bonds in the cementite lattice, both of which increase the stability of cementite and its resistance to dissolution upon the deformation imposed by wear [24,28,29]. Other elements such as Mn, Cr, and B have been found to increase the hardness and stability of cementite, as opposed to Si, Co, and Ni, which decrease it [30]. In order to confirm the alleged change in mechanical properties of vanadium containing cementite compared to conventional cementite, microindentation was performed after spheroidising samples of R290V and R290GHT in a dilatometer at 680 °C for 72 h in order to create larger carbides easier to indent. The results shown in Table 3 confirm the reduction in hardness of vanadium alloyed cementite, which should increase toughness and the resistance of cementite to deformation-induced dissolution.

3.2. Twin disc wear testing

The results of twin disc wear testing are presented in Fig. 5. It is worth noting that the wear rates of the wheel discs (Fig. 5) are approximately proportional to the hardness of the rail disc as found by other authors in cases of early stages of wear and constant slip [31–33]. Furthermore, the total average wear rate of the system remains more or less constant between 12 and 13 mg kcycle^{-1}, with the exception of the R290GHT-R7 system, confirming the findings of Markov, who pointed out that the total wear rate is relatively independent of hardness under

[1] The equilibrium transformation temperature increases 1 °C per 0.1 wt% of Cr and 2.4 °C for each 0.1 wt% of Si in a 0.8 wt% C steel [25], which raises the amount of supercooling with respect to the pearlite transformation-start temperature, thus refining the interlamellar spacing and increasing the hardness.

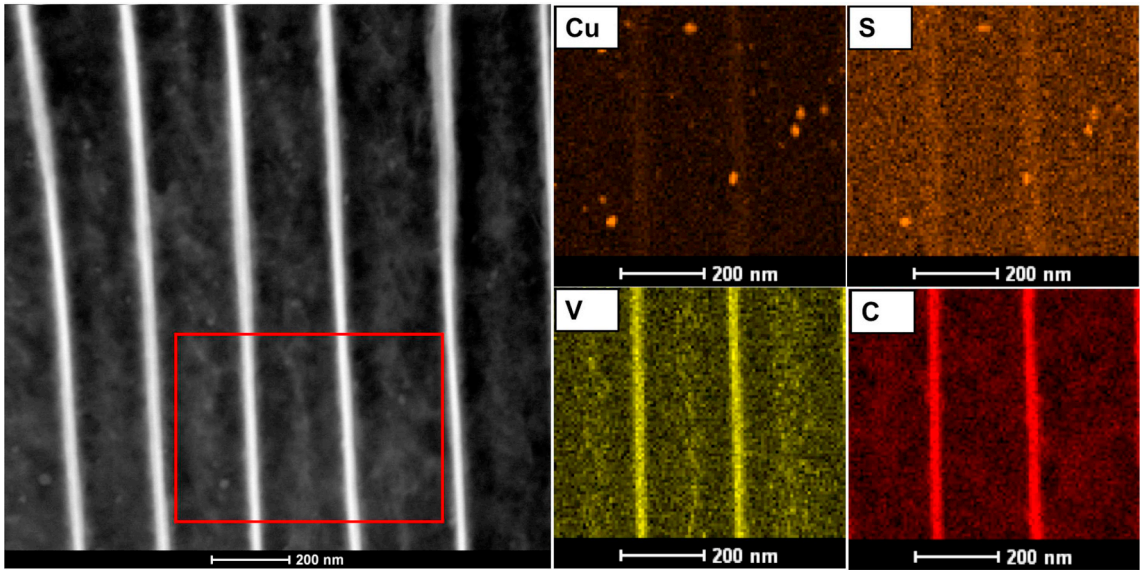

Fig. 2. HAADF micrograph of lamellar pearlite in R290V and associated EDX elemental maps of the area marked by a red rectangle (For interpretation of the references to colour in this figure legend, the reader is referred to the Web version of this article.)

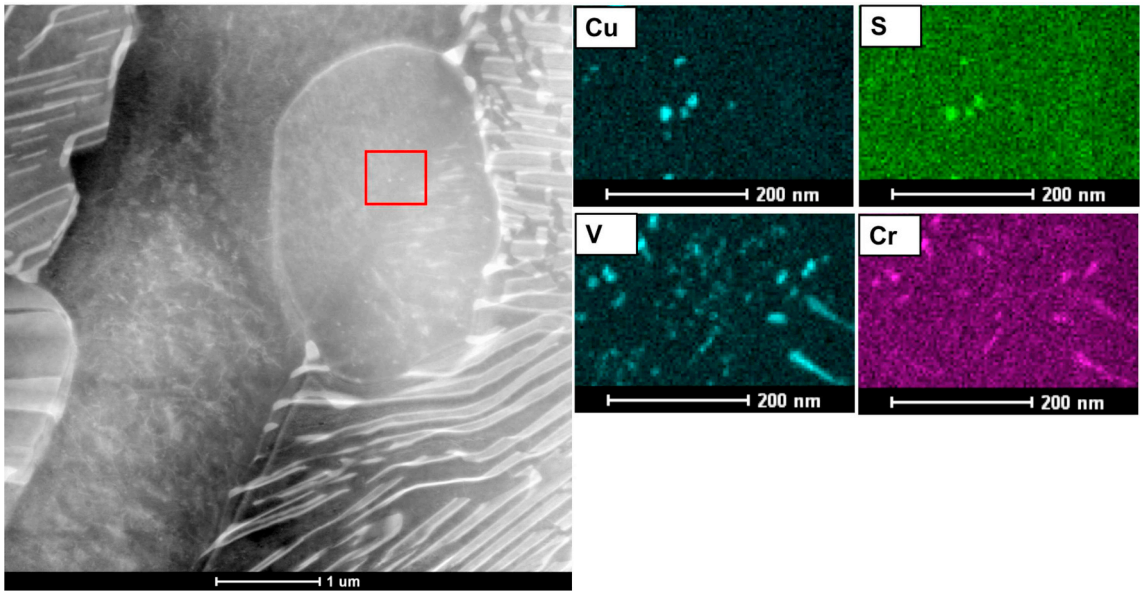

Fig. 3. HAADF micrograph of a proeutectoid ferrite region in R290V and associated EDX elemental maps of the area marked by a red rectangle (For interpretation of the references to colour in this figure legend, the reader is referred to the Web version of this article.)

mild wear conditions (slip below 5%) because the fatigue component redistributes plastic deformation at the surface of the discs.

The most interesting observation is that at identical hardness, but a coarser interlamellar spacing, R290V shows *less than half* the wear rate of its counterpart, R290GHT. Nevertheless, both the weldability,[2] based on the carbon equivalent (Table 4), and wear rate of the wheel disc are comparable for both steels. As discussed in the previous section, vanadium was not found to refine the prior austenite grain size or create a high density of fine precipitates in the pearlitic ferrite, thus suggesting that it is the higher toughness and stability of the cementite containing vanadium that is responsible of this high wear resistance of R290V compared to the unalloyed cementite in R290GHT. The high carbon alloys, B1000 and R340GHT, show comparable values of rail and wheel wear rates, since their rolling-surface hardness and sub-surface interlamellar spacing are similar. They both offer a somewhat higher wear resistance than R290V, but roughly a threefold improvement with respect to R290GHT; the only caveat being their reduced weldability. This is important because high wear-resistance grades are not used for the whole tramway but in specific locations such as tight curves or shallow curves/tangent track, where vertical wear is dominant, thus necessitating of easy welding and repair protocols.

To analyse the influence of the other solutes, different wear rate equations were used to interpret the data of this study [2,3]. The results indicate that the current rail wear data correlate more accurately to chemical composition than to the interlamellar spacing or mean free path in ferrite, thus explaining the 2.3 times lower wear rate of R290V than R290GHT despite a larger interlamellar spacing [2,3]. The chemical composition model for wear rate based on the amounts of C, Mn, and Si of an alloy, predicts accurately the lowest wear rates for B1000 and R340GHT and the highest for R290GHT, with R260 and R290V in

[2] A separate study dedicated to the weldability of these alloys is being prepared.

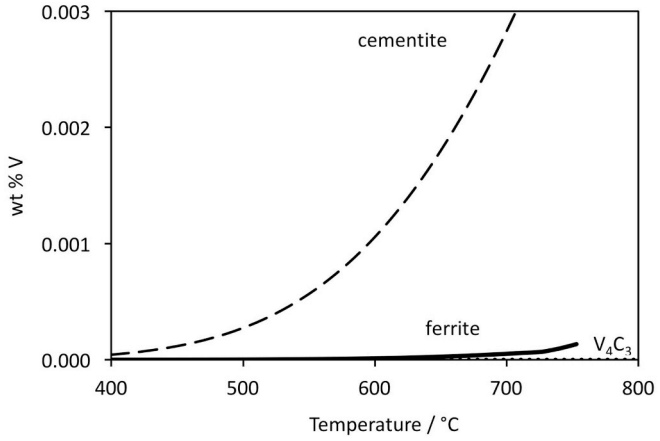

Fig. 4. Thermodynamic simulation using Thermo-Calc of the elemental composition of vanadium in the different phases in R290V as a function of temperature.

Table 3
Microhardness of spheroidised cementite in R290V and R290GHT, based on 40 indentations of cementite globules in each sample with a load of 0.5 g.

Grade	Hardness cementite/HV	
	average	maximum
R290V	837±115	1801
R290GHT	1133±178	2318

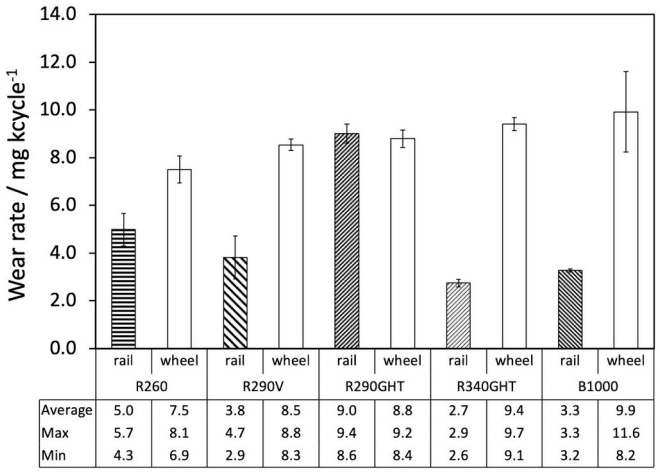

Fig. 5. Results of unlubricated twin disc wear tests that ran for 100,000 cycles at room temperature and 750 MPa of contact pressure using grade R7 for all wheel discs. Two samples were tested per composition.

Table 4
Rail wear rate summary, carbon equivalent, and a schematic of the balance between wear and weldability of the alloys studied.

Grade	Wear rate/ mg kcycle^{-1}	Carbon equivalent	Wear resistance	Weldability	Overall score
R260	5.0±1.3	0.8	**	**	4
R290V	3.8±1.8	0.7	**	***	5
R290GHT	9.0±0.8	0.6	*	***	4
R340GHT	2.7±0.3	0.9	***	*	4
B1000	3.3±0.1	0.9	***	*	4

the middle range. Instead, equations that correlate wear rate to either the mean true interlamellar spacing or ferrite free mean path, fail to replicate the high wear rates of R290GHT, whilst giving instead high values of wear for R260 and R290V.[3] These results do not imply that the chemical composition has a greater influence on wear that hardness, but attempt to understand which other factor, composition or heat treatment, plays a greater role in improving the wear resistance beyond a base level imparted by a certain hardness.

A summary of the average rail wear values and standard errors with a 95% confidence interval along with a schematic of wear resistance and perceived weldability based on carbon equivalent[4] for the alloys studied here is presented in Table 4, where * is the lowest and *** for the highest, along with an overall score ranging from 1 to 6, where 1 is the lowest and 6 the highest possible score based on the sum of these two parameters only. It is worth pointing out that the ranking is a rough guide of the balance between wear and weldability and does not take into account other life cycle costs or resistance to other damage mechanisms.

4. Conclusions

The following conclusions can be drawn for the evidence presented:

- R290V displays *less than half* the wear rate of an alloy with similar hardness, R290GHT, despite having a higher true interlamellar spacing. For the specific rolling and cooling conditions of the alloys studied in this work, vanadium does not seem to play a role as a grain refiner. Instead, the higher toughness and stability of the cementite enhanced with vanadium is thought to be responsible of the 2.3 higher wear resistance of R290V compared to R290GHT, containing regular cementite. Such improvement of wear rate resistance in R290V could reduce by more than half the maintenance and life cycle costs of a tramway compared to R290GHT or by approximately a third when compared against standard R260 steel.
- According to microscopical observations and thermodynamic simulations, the mechanism by which vanadium enhances the wear behaviour of pearlite in R290V is revealed. It consists of vanadium enrichment of the cementite lamellae by partitioning into the iron carbide during the pearlitic transformation, product of the cooling conditions after rolling.
- By precise alloying with the right amounts of C, Cr, and V, the alloy B1000 achieves comparable values of hardness, prior austenite grain size, true interlamellar spacing, and wear rate (of both the rail and wheel discs) as the high carbon head hardened (fast cooled) alloy R340GHT.

Acknowledgements

The authors acknowledge and appreciate the contributions of Gebril El-Fallah of Cambridge University for help with TEM sample preparation, Dr Giorgio Divitini of Cambridge University for TEM EDX analysis, Maria Panera of IDONIAL for support with twin disc testing, Jesus Alberto Garcia Ferreno of IDONIAL for microhardness measurements, Felipe Alvarez of IDONIAL for machining samples, Jose Manuel Artimez Encina of IDONIAL and Jose Arancon Alvarez of ArcelorMittal for comments and discussion, David Alvarez Diez of ArcelorMittal for providing samples, and Javier Somoano of ArcelorMittal for engineering drawings. This work was financed by the University of

[3] 1) wear rate [mm^3 cm^{-1}] = 0.0708 $log\lambda_\alpha$ + 0.0329, where λ_α is the mean free path in ferrite [2]. 2) wear rate [mm^3 cm^{-1}] = −0.1427 wt%*(C + Mn/4.75 + Si/10)+ 0.1605 [2]. 3) wear rate (700 MPa) [μg m^{-1}] = 7.97*$S^{1.51}$, where S is the mean true interlamellar spacing [3].

[4] using CET from EN 1011–2:2003 [34,35], which matches the result of the CEw formula that takes vanadium into account [36].

Cambridge and ArcelorMittal Research Collaboration Agreement number 6085701156.

References

[1] A. Bevan, J. Jaiswal, A. Smith, M.O. Cabral, Judicious selection of available rail steels to reduce life-cycle costs, Proceedings of the Institution of Mechanical Engineers, Part F, J. Rail Rapid Transit (2018), https://doi.org/10.1177/0954409718802639.

[2] P. Clayton, The relations between wear behaviour and basic material properties for pearlitic steels, Wear 60 (1980) 75–93.

[3] P. Clayton, D. Danks, Effect of interlamellar spacing on the wear resistatnce of eutectoid steels under rolling–sliding conditions, Wear 135 (1990) 369–389.

[4] F.P.L. Kavishe, T.J. Baker, Effect of prior austenite grain size and pearlite interlamellar spacing on strength and fracture toughness of a eutectoid rail steel, Mater. Sci. Technol. 2 (8) (1986) 816–822.

[5] R. Heyder, G. Girsch, Testing of HSH® rails in high-speed tracks to minimise rail damage, Wear 258 (7) (2005) 1014–1021.

[6] G.G. Knupp, W.H. Chidley, J.L. Glove, H.H. Hartman, G.F. Morris, C.W. Taylor, A review of the manufacture, processing, and use of rail steels in north America- a report of aisi technical subcommittee on rails and accessories, Rail Steels–Developments, Processing, and Use: A Symposium, vol. 644, ASTM International, 1976, p. 7.

[7] F.B. Pickering, B. Garbarz, Strengthening in pearlite formed from thermo-mechanically processed austenite in vanadium steels and implications for toughness, Mater. Sci. Technol. 5 (3) (1989) 227–237.

[8] G.L. Dunlop, C.-J. Carlsson, G. Frimodig, Precipitation of vc in ferrite and pearlite during direct transformation of a medium carbon microalloyed steel, Metall. Mater. Trans. A 9 (1978) 261–266.

[9] A. von den Steinen, S. Engineer, E. Horn, G. Preis, Investigations of steels with about 0.5C and small addition of vanadium and niobium, Stahl Eisen 95 (6) (1975) 209–214.

[10] S.A. Parsons, D.V. Edmonds, Microstructure and mechanical properties of medium-carbon ferrite-pearlite steel microalloyed with vanadium, Mater. Sci. Technol. 3 (11) (1987) 894–904.

[11] F. Katsuki, M. Yonemura, Subsurface characteristics of an abraded Fe-0.4 wt%C pearlitic steel: a nanoindentation study, Wear 263 (2007) 1575–1578.

[12] F. Katsuki, K. Watari, H. Tahira, M. Umino, Abrasive wear behavior of a pearlitic (0.4%C) steel microalloyed with vanadium, Wear 264 (2008) 331–336.

[13] S.W. Thompson, G. Krauss, Precipitation and fine structure in a medium-carbon vanadium and vanadium/niobium microalloyed steels, Metall. Trans. A 20 (11) (1989) 2279–2288.

[14] A.T. Davenport, F.G. Berry, R.W.K. Honeycombe, Interphase precipitation in iron alloys, Met. Sci. 2 (1968) 104–106.

[15] A.T. Davenport, R.W.K. Honeycombe, Precipitation of carbides at γ–α boundaries in alloy steels, Proc. R. Soc. Lond. 322 (1971) 191–205.

[16] K. Han, T.D. Mottishaw, G.D.W. Smith, D.V. Edmonds, Effects of vanadium addition on nucleation and growth of pearlite in high carbon steel, Mater. Sci. Technol. 10 (11) (1994) 955–963.

[17] K. Han, T.D. Mottishaw, G.D.W. Smith, D.V. Edmonds, A.G. Stacey, Effects of vanadium additions on microstructure and hardness of hypereutectoid pearlitic steels, Mater. Sci. Eng. A 190 (1995) 207–214.

[18] Railway Applications – Track - Special Purpose Rail - Grooved and Associated Construction BS EN 14811, (2009) 2006 + A1.

[19] E.E. Underwood, Quantitative Stereology, Addison–Wesley Publication Company, 1970.

[20] G.F. Vander Voort, A. Roósz, Measurement of the interlamellar spacing of pearlite, Metallography 17 (1984) 1–17.

[21] EN ISO 6506-1 Metallic Materials—Brinell Hardness Test- Part 1, (2005).

[22] R. Ordóñez-Olivares, C.I. García, A. DeArdo, S. Kalay, F.C. Robles-Hernández, Advanced metallurgical alloy design and thermomechanical processing for rails steels for north american heavy haul use, Wear 271 (1) (2011) 364–373.

[23] Anonymous, The Effect of Carbide Network on the Life of AISI 52100 in Rolling Contact Fatigue, Tech. Rep. May 6 Federal–Mogul Corporation, Derbyshire, U. K., 1982.

[24] W. Solano-Alvarez, M.J. Peet, E.J. Pickering, J. Jaiswal, A. Bevan, H.K.D.H. Bhadeshia, Synchrotron and neural network analysis of the influence of composition and heat treatment on the rolling contact fatigue of hypereutectoid pearlitic steels, Mater. Sci. Eng., A 707 (2017) 259–269.

[25] K. Tokunaga, T. Arimura, M. Yamaguchi, H. Fukuda, M. Honjo, R. Matsuoka, M. Takemasa, Development of SP4 rail with high wear resistance for heavy haul railways, Tech. rep., JFE steel (2017).

[26] J.O. Andersson, T. Helande, L. Hoglund, P. Shi, B. Sundman, Thermo-Calc & DICTRA, computational tools for materials science, Calphad 26 (2002) 273–312.

[27] J.J. Coronado, S.A. Rodrguez, Cementite characterization with chromium and vanadium contents using indentation technique, J. Iron Steel Res. Int. 22 (4) (2015) 366–370.

[28] I.R. Shein, N.I. Medvedeva, A.L. Ivanovskii, Electronic structure and magnetic properties of Fe3C with 3d and 4d impurities, Phys. Status Solidi B 244 (6) (2007) 1971–1981.

[29] V.G. Gavriljuk, Decomposition of cementite in pearlitic steel due to plastic deformation, Mater. Sci. Eng., A 345 (2003) 81–89.

[30] H.K.D.H. Bhadeshia, Cementite, Int. Mater. Rev. (2019), https://doi.org/10.1080/09506608.2018.1560984.

[31] D. Markov, Laboratory tests for wear of rail and wheel steels, Wear 181 (1995) 678–686.

[32] Y. Jin, M. Ishida, A. Namura, Experimental simulation and prediction of wear of wheel flange and rail gauge corner, Wear 271 (1) (2011) 259–267.

[33] R.K. Steele, R.P. Reiff, Rail: its behaviour and relationship to total system wear, Proceedings of the Second International Heavy Haul Railway Conference, 1982, pp. 115–164 Colorado Springs, Colorado, USA.

[34] British Standards Institution, Welding- Recommendations for welding metallic materials- Part 2: Arc welding of ferritic steels, Tech. Rep. (2003).

[35] N. Yurioka, Carbon equivalents for hardenability and cold cracking susceptibility of steels, Select Conference on Hardenability of Steels, Vol. Paper 3 17 May 1990 Derby, UK.

[36] C.L. Cottrell, An improved prediction method for avoiding HAZ hydrogen cracking, Weld. Metal Fabr. 58 (3) (1990) 178–183.